NMR diffusion spectroscopy for the characterization of multicomponent hydrogen-bonded assemblies in solution

Peter Timmerman,*[a] Jean-Luc Weidmann,[a] Katrina A. Jolliffe,[a] Leonard J. Prins,[a] David N. Reinhoudt,*[a] Seiji Shinkai,[b] Limor Frish[c] and Yoram Cohen*[c]

[a] *Laboratory of Supramolecular Chemistry and Technology, MESA$^+$ Research Institute, University of Twente, PO Box 217, 7500 AE, Enschede, The Netherlands*
[b] *Chemotransfiguration Project, Japan Science and Technology Corporation, 2432 Aikawa, Kurume, Fukuoka 839-0861, Japan*
[c] *School of Chemistry, The Sackler Faculty of Exact Sciences, Tel Aviv University, Ramat Aviv 69978, Tel Aviv, Israel*

Received (in Cambridge, UK) 17th May 2000, Accepted 11th July 2000
Published on the Web 31st August 2000

NMR diffusion measurements on 10 different multicomponent hydrogen-bonded assemblies, *viz.* the three single rosettes **SR1–SR3** (**1**$_3$·**2a**$_3$, **1**$_3$·**2b**$_3$, **1**$_3$·**2c**$_3$) the double rosettes **DR1–DR5** (**3a**$_3$·**2a**$_6$, **3b**$_3$·**2b**$_6$, **3c**$_3$·**2a**$_6$, **3d**$_3$·**2a**$_6$, **3e**$_3$·**2a**$_6$), and **DR6** (**4a**$_3$·**1**$_6$), and the tetrarosette **TR** (**5**$_3$·**2a**$_{12}$) are described. Some of the above rosettes have been previously identified as well-defined assemblies (*viz.* **SR1**, **DR1–DR3**, and **TR**) using established characterization techniques (^{1}H NMR spectroscopy, X-ray diffraction, and MALDI-TOF MS after Ag$^+$-labeling). The diffusion coefficients of these assemblies were studied and used as a reference for the identification of three new assemblies (**DR4–DR6**), the characterization of which could not be established unequivocally using other characterization tools. A good correlation was found between the experimental and calculated diffusion coefficients when **DR1** was used as a reference. A relatively good correlation was obtained between the effective hydrolytic radii calculated from the diffusion data and those extracted from gas phase-minimized structures with **SR1** and **DR2** being exceptions. The diffusion measurements show that assembly **DR4** is a thermodynamically stable species, while assemblies **DR5** and **DR6** are less stable and only present to a minor extent.

Introduction

Multiple hydrogen bond formation has opened a synthetically useful way to assemble individual molecular components into functional organic nanostructures that are held together in a reversible manner.[1] Molecules containing the correct structural information spontaneously assemble into helices,[2] rosettes,[1] cylinders,[3] capsules,[4–6] dendrimers,[7] polymers,[8,9] or grids.[10] The structural characterization of such assemblies often relies on a combination of data obtained from techniques like ^{1}H NMR spectroscopy, X-ray diffraction, mass spectrometry and vapor pressure osmometry (VPO). While most of these techniques are suitable for the characterization of monodisperse assemblies of well-defined composition, few techniques provide structural information about the identity of assemblies in polydisperse mixtures. Recently, it was demonstrated that NMR diffusion measurements, as obtained from the pulsed gradient spin echo (PGSE) technique,[11] is a useful method for the characterization of a variety of organic supramolecular systems in solution.[12] Furthermore, diffusion ordered NMR spectroscopy (DOSY) has been proposed for studying mixtures of compounds.[13a–c] High resolution DOSY (HR-DOSY) has been developed[13d,e] and PGSE experiments were very recently used to probe the structure of a 50-component dodecahedra and some cyclodextrin-based complexes and rotaxanes.[12g–i] We have now studied this technique as a potential method for the characterization of hydrogen-bonded rosette assemblies in solution. The results of these studies are described in this paper.

Results and discussion

The noncovalent synthesis of discrete planar hydrogen-bonded assemblies using multivalent interactions between covalently preorganized cyanuric acid† and melamine† derivatives was largely developed by Whitesides *et al.*[1] Inspired by this work we explored the noncovalent assembly of a variety of calix[4]arene double rosette assemblies **3**$_3$·**2**$_6$ (**DR**)[14] and tetrarosette assemblies **5**$_3$·**2**$_{12}$ (**TR**).[15] The calix[4]arene units are an essential structural element of these assemblies, because they promote the exclusive formation of cyclic double rosette assemblies in favor of other polydisperse oligomeric assemblies. As a result these assemblies are thermodynamically stable in a wide concentration range (10^{-1}–10^{-4} M) in apolar solvents. In the present study we describe NMR diffusion measurements with four different types of rosette assemblies, *i.e.* single rosettes **SR1–SR3** (**1**$_3$·**2a**$_3$, **1**$_3$·**2b**$_3$, **1**$_3$·**2c**$_3$), double rosettes **DR1–DR5** (**3a**$_3$·**2a**$_6$, **3b**$_3$·**2b**$_6$, **3c**$_3$·**2a**$_6$, **3d**$_3$·**2a**$_6$, **3e**$_3$·**2a**$_6$), double rosette **DR6** (**4a**$_3$·**1**$_6$), and tetrarosette **TR** (**5**$_3$·**2a**$_{12}$) (see Fig. 1, Table 1). The single rosette **SR1**, **DR1–DR3**, and **TR**, (entries 1, 4–6, and 10, Table 1) have been previously characterized as monodisperse assemblies of well-defined composition using established techniques (^{1}H NMR spectroscopy, X-ray crystal diffraction, MALDI-TOF MS, and CD spectroscopy). The diffusion coefficients of several systems namely **SR1**, **DR1–3** and **TR** were used as references to obtain anticipated diffusion coefficients of the other systems. The experimental diffusion coefficients were used to calculate hydrolytic radii, which were then compared with the calculated radii obtained from gas phase-minimized structures. This procedure assisted us in the assignment of the structure and the nature of three other assemblies (*i.e.* **DR4–DR6**), for which our standard set of characterization

† IUPAC names for cyanuric acid, melamine, barbituric acid and phthalimide are 1,3,5-triazine-2,4,6-triol, 2,4,6-triamino-1,3,5-triazine, pyramidine-2,4,6-triol and isoindoline-1,3-dione, respectively.

DOI: 10.1039/b003968n

Table 1 Diffusion coefficients (D_{exp}) determined using the pulsed gradient spin echo (PGSE) technique and effective experimental (r_{exp}) and calculated (r_{calc}) hydrolytic radii for the hydrogen-bonded assemblies **SR1–3**, **DR1–6**, and **TR**

Entry	Assembly	D_{exp}[a,b]/10^{-5} cm^2 s^{-1}	M_r	r_{exp}[c]/Å	r_{calc}[d] [0.5(h + d + l)/3]/Å
1	$\mathbf{1_3{\cdot}2a_3}$ **(SR1)**	0.55 ± 0.01	1723	7.3 ± 0.2	9.7 [0.5(28 + 24 + 6)/3]
2	$\mathbf{1_3{\cdot}2b_3}$ **(SR2)**	0.47 ± 0.02	1870	8.4 ± 0.5	9.8 [0.5(28 + 24 + 7)/3]
3	$\mathbf{1_3{\cdot}2c_3}$ **(SR3)**	0.48 ± 0.02	2371	8.4 ± 0.5	10.2 [0.5(28 + 24 + 9)/3]
4	$\mathbf{3a_3{\cdot}2a_6}$ **(DR1)**	0.34 ± 0.01	4235	11.8 ± 0.4	11.8 [0.5(32 + 27 + 12)/3]
5	$\mathbf{3b_3{\cdot}2b_6}$ **(DR2)**	0.28 ± 0.01	4462	14.4 ± 0.5	12.2[e] [0.5(32 + 26 + 15)/3]
6	$\mathbf{3c_3{\cdot}2a_6}$ **(DR3)**	0.32 ± 0.01	4170	12.6 ± 0.4	12.3 [0.5(32 + 26 + 16)/3]
7	$\mathbf{3d_3{\cdot}2a_6}$ **(DR4)**	0.33 ± 0.02	4319	12.2 ± 0.4	12.0 [0.5(33 + 27 + 12)3]
8	$\mathbf{3e_3{\cdot}2a_6}$ **(DR5)**	0.37 ± 0.01[f]	3628	10.9 ± 0.3	10.7 [0.5(27 + 25 + 12)/3]
9	$\mathbf{4a_3{\cdot}1_6}$ **(DR6)**	0.29 ± 0.01	4966	13.9 ± 0.5	13.0 [0.5(30 + 30 + 18)/3]
10	$\mathbf{5_3{\cdot}2a_{12}}$ **(TR)**	0.27 ± 0.01	7899	14.9 ± 0.5	14.7 [0.5(33 + 33 + 22)/3]

[a] Since the diffusion coefficients of chloroform were slightly different for different samples, the ratios between the theoretical diffusion coefficients of chloroform (2.35×10^{-5} cm^2 s^{-1}) and the experimental diffusion coefficients were used to correct the experimental values. [b] All NMR diffusion measurements were performed on 2 mM samples in $CDCl_3$ at 298 K. [c] For spheres diffusing in a medium of viscosity η, the relation between the diffusion coefficient D and the effective radius of the sphere R is given by the Stokes–Einstein equation: $R = k_bT/6\pi\eta D$ where k_b is the Boltzmann constant and T is the absolute temperature. The viscosity of chloroform, η(25 °C) = 0.542 cp was used. [d] Calculated values were determined by averaging the radius in the x, y, and z-direction of the gas phase-minimized structures from Fig. 3. [e] This r value depends strongly on the relative orientation of the phenyl side chains. [f] Based on a single peak at 3.72 ppm representing the OMe group of only one of the species in the solution.

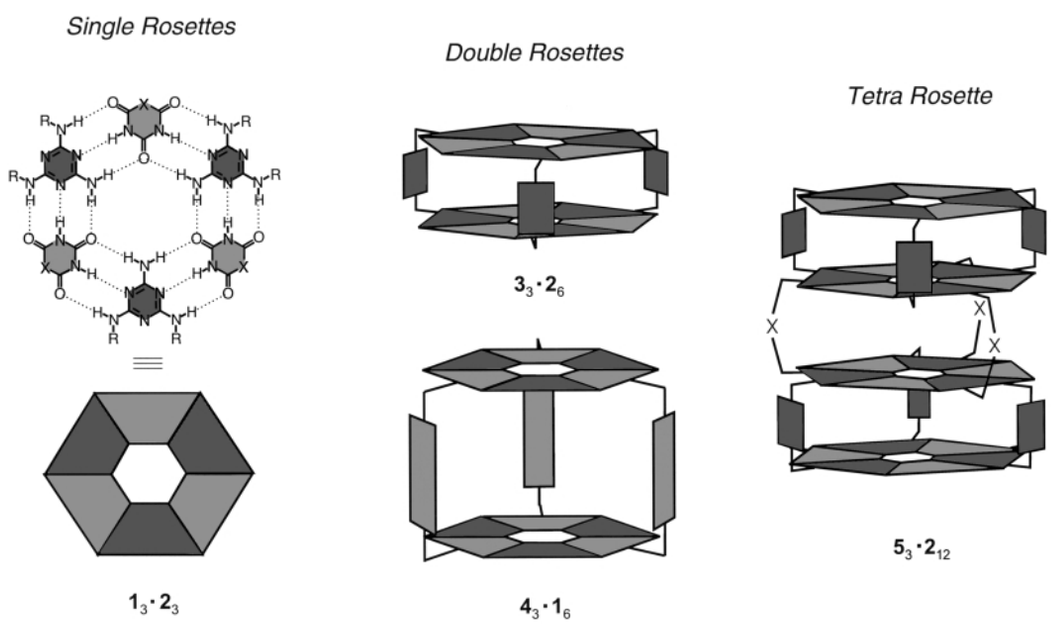

Fig. 1 Chemical structure and schematic representation of single rosette assembly $\mathbf{1_3{\cdot}2_3}$, double rosette assemblies $\mathbf{3_3{\cdot}2_6}$ and $\mathbf{4_3{\cdot}1_6}$, and tetrarosette assembly $\mathbf{5_3{\cdot}2_{12}}$.

techniques so far did not give conclusive evidence about their identity and/or uniformity.

The diffusion coefficients (D) for each assembly were measured using the PGSE technique in $CDCl_3$ at 298 K and are given in Table 1. Fig. 2 shows the signal intensity decay curves as a function of the b value [$b = \gamma^2\delta^2g^2(\Delta - \delta/3)$, where γ = gyromagnetic radius (rad s^{-1} G^{-1}), δ = length of the diffusion gradients (s), g = gradient strength of the diffusion gradients (G cm^{-1}) and Δ = time separation between the gradients (s)] for **SR1**, **DR1** and **TR** from which the diffusion coefficients (D_{exp}) were determined. The high accuracy of these measurements ($\pm 0.01 \times 10^{-5}$ cm^2 s^{-1}) clearly shows that the resolution of the PGSE technique is sufficient to distinguish between assemblies with different molecular weight (M_r). The single rosette assemblies (**SR**) with diffusion coefficients (D_{exp}) in the range of (0.47–0.55 ± 0.02) $\times 10^{-5}$ cm^2 s^{-1} can be easily distinguished from the double rosettes (**DR**), whose diffusion coefficients are in the range of (0.28–0.34 ± 0.01) $\times 10^{-5}$ cm^2 s^{-1}. At first glance, distinguishing between the double (**DR**) and the tetrarosette assemblies (**TR**) seems to be more difficult. However, for a useful comparison of these data it is necessary to understand the relation between M_r and the diffusion coefficient of a particular assembly. It should be realized that the shape of

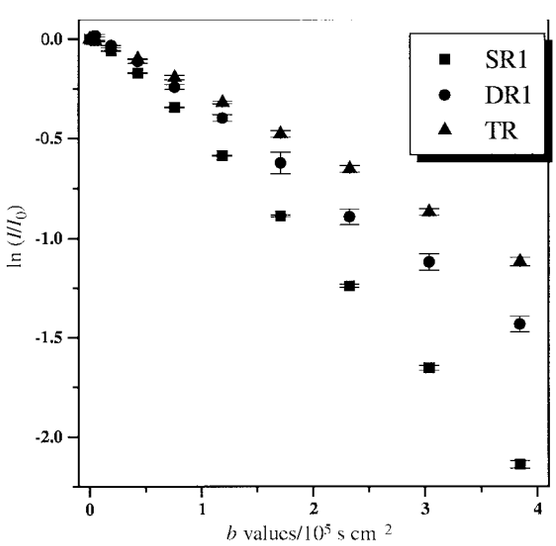

Fig. 2 Natural logarithm of the normalized signal intensity for single rosette assembly $\mathbf{1_3{\cdot}2a_3}$ (■), double rosette assembly $\mathbf{3a_3{\cdot}2a_6}$ (●) and tetrarosette assembly $\mathbf{5_3{\cdot}2a_{12}}$ (▲) as a function of b values ($b = \gamma^2\delta^2g^2(\Delta - \delta/3)$). The slope of these lines is equal to $-D$.

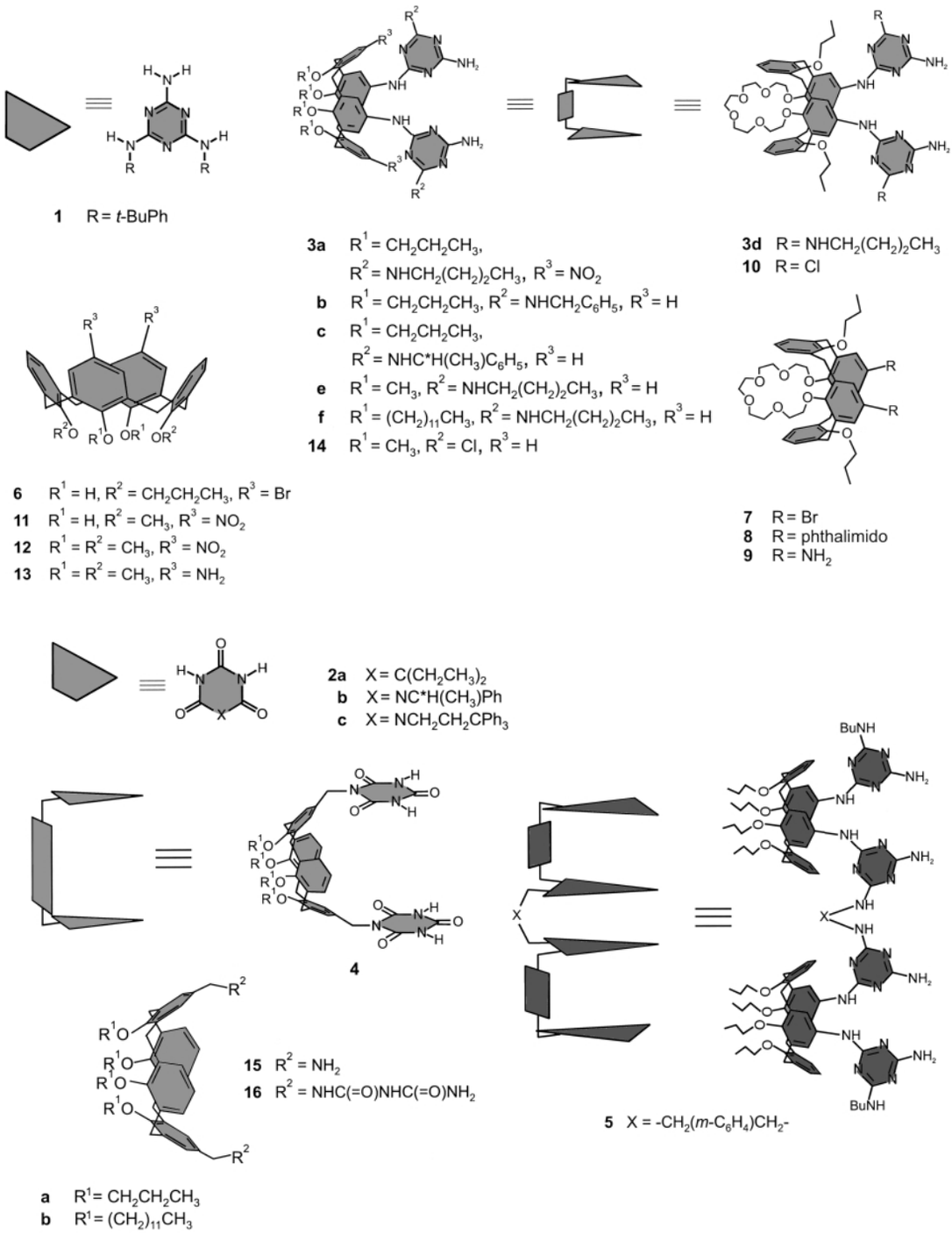

a given molecular species can significantly affect the relation between M_r and the diffusion coefficient, which can complicate a direct comparison of the data. Therefore, we have analyzed the diffusion coefficients of the various assemblies in two different ways, either by comparison of the experimental data with expected (*i.e.* calculated) diffusion coefficients (see Table 2), or by comparison of the corresponding Stokes radii with the average radii as determined from gas phase-minimized structures (see Fig. 3).

The first analysis of the diffusion data involves the correlation of the experimental diffusion coefficients with calculated values that are corrected for the difference in molecular weight. It has been claimed that the ratio of diffusion coefficients for two different molecular species (D_i/D_j) is inversely proportional to the square-root or to the cubic-root of the ratio of their M_r [eqn. (1)] for rod-like and spherical molecules, respectively.[16]

$$\sqrt[3]{\frac{[M_{rj}]}{[M_{ri}]}} \leq \frac{[D_i]}{[D_j]} \leq \sqrt{\frac{[M_{rj}]}{[M_{ri}]}} \qquad (1)$$

Using this relation one can calculate a set of theoretical diffusion coefficients (D_{calc}) (upper and lower limit) for each assembly using the D_{exp} of any other assembly as a reference. The calculated data using the D_{exp} values of assemblies **SR1**, **DR1–DR3**, and **TR** as references are given in Table 2. In order to support a meaningful interpretation of these data we have added Fig. 4.

Secondly, we calculated the hydrolytic (Stokes) radius r_{exp} for each assembly from the D_{exp} values using the Stokes–Einstein equation (assuming spherical shape of all the assemblies) and compared these values with the average radius (r_{calc} = average of x, y, and z values) of the corresponding gas phase-minimized structures (see Fig. 3). Both r_{exp} and r_{calc} values are also listed in Table 1.

Table 2 Calculated range (upper and lower limit) of self-diffusion coefficients (D_{calc}) for assemblies **SR1–3**, **DR1–DR6**, and **TR** using the D_{exp} of **SR1**, **DR1–DR3**, and **TR** as a reference value[a]

Ass.	D_{calc} relative to **SR1**/10^{-5} cm^2 s^{-1}	D_{calc} relative to **DR1**/10^{-5} cm^2 s^{-1}	D_{calc} relative to **DR2**/10^{-5} cm^2 s^{-1}	D_{calc} relative to **DR3**/10^{-5} cm^2 s^{-1}	D_{calc} relative to **TR**/10^{-5} cm^2 s^{-1}
SR1	—	0.46–0.55	0.38–0.45	0.43–0.50	0.45–0.58
SR2	0.53–0.54	0.45–0.51	0.37–0.43	0.42–0.48	0.44–0.55
SR3	0.47–0.49	0.41–0.45	0.35–0.38	0.39–0.42	0.40–0.49
DR1	0.35–0.41	—	0.28–0.29	~0.32	0.33–0.37
DR2	0.34–0.40	~0.33	—	~0.31	0.33–0.36
DR3	0.35–0.41	~0.34	~0.29	—	0.33–0.37
DR4	0.35–0.40	~0.34	~0.28	0.31–0.32	0.33–0.37
DR5	0.38–0.43	0.36–0.37	0.30–0.31	~0.34	0.35–0.40
DR6	0.32–0.39	0.31–0.32	~0.27	0.29–0.30	0.32–0.34
TR	0.26–0.33	0.25–0.28	0.21–0.23	0.23–0.26	—

[a] Diffusion coefficients were calculated according to eqn. (1).

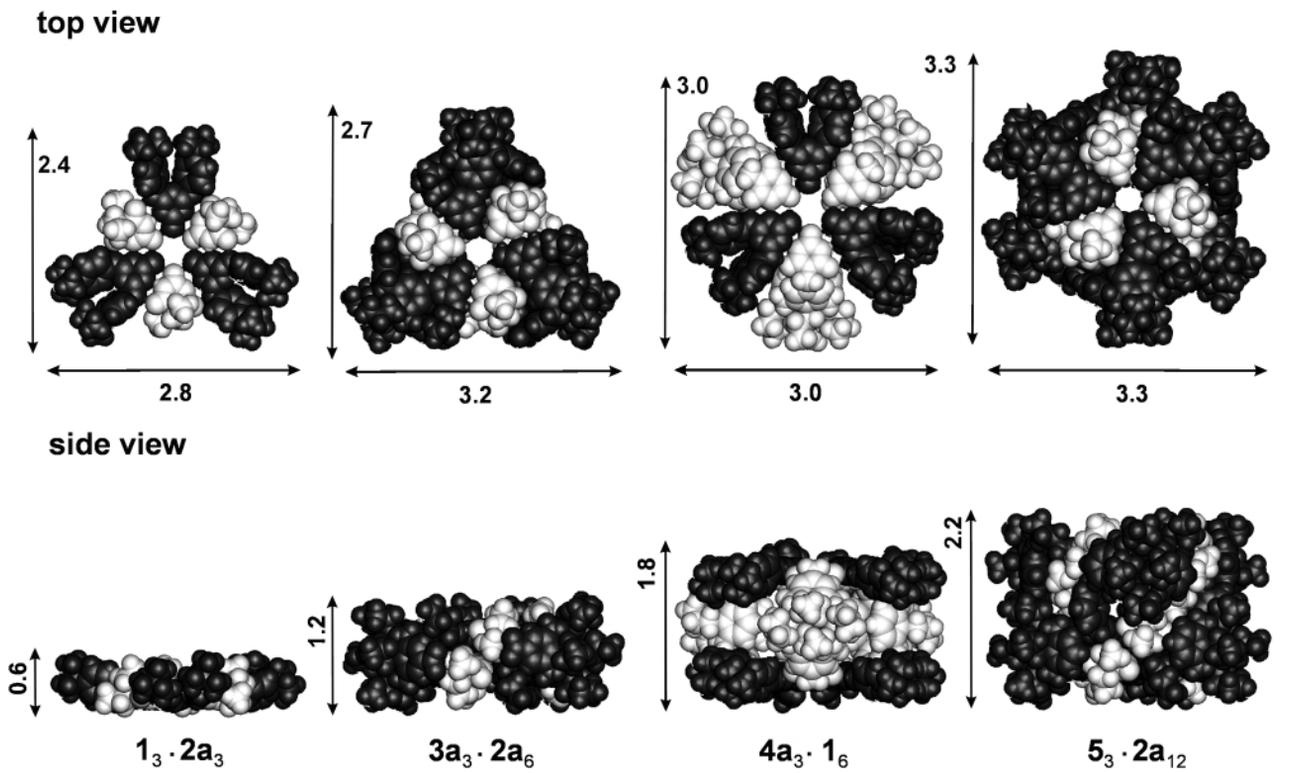

Fig. 3 Gas phase-minimized structure and dimensions (nm) of single rosette assembly $\mathbf{1_3 \cdot 2a_3}$ (**SR1**), double rosette assemblies $\mathbf{3a_3 \cdot 2a_6}$ (**DR1**) and $\mathbf{4a_3 \cdot 1_6}$ (**DR6**), and tetrarosette assembly $\mathbf{5_3 \cdot 2a_{12}}$ (**TR**).

From the data in Tables 1 and 2 the following general trends emerge. (1) The best correlation between experimental and calculated diffusion coefficients was found when **DR1** was used as a reference. (2) There is a relatively good agreement between the hydrolytic radii extracted from the diffusion data (r_{exp}) and from the gas phase-minimized structures (r_{calc}) (the only exception being **DR2** and **SR1**). (3) The correlation between the D_{calc} and the D_{exp} values is much weaker when **TR** is used as a reference compound (large difference in M_r with other assemblies). (4) The D_{calc} values for **SR1** (and also **SR3**) are much lower than the D_{exp} values when **DR1–3** are used as references. Similarly, the D_{exp} values for **DR1–DR3** are all outside the range of D_{calc} values when **SR1** is used as a reference.

The deviation of the **SR1** data most likely originates from the relatively low thermodynamic stability of single rosettes, which decompose significantly at concentrations below 10^{-2} M in chloroform.[17] The diffusion coefficients as determined for assembly **SR1** therefore represent a weighted average for the intact assembly and the free components **1** and **2a**. Supportive evidence for this view was obtained from diffusion measurements on solutions of assembly **SR1** to which an excess of **2a** was added. The decay of the signal for **2a** was found to be mono-exponential and the extracted diffusion coefficient was $(0.93 \pm 0.02) \times 10^{-5}$ cm^2 s^{-1}, much larger than the value obtained with a stoichiometric amount of **2a**. This experiment clearly indicates that assembly **SR1** is in fast exchange with its components on the diffusion NMR timescale. Interestingly, the diffusion coefficients of **SR2** and **SR3** [$(0.47 \pm 0.02) \times 10^{-5}$ cm^2 s^{-1}] are somewhat smaller than that of **SR1**. This difference most likely reflects the increase in hydrogen bond strength for cyanurates (**2b** and **2c**) in comparison to barbiturates† (**2a**).[18] When the NMR diffusion experiments were performed with assembly **DR1** to which an excess of **2a** was added, the result was different. In this case the signals of **2a** showed bi-exponential decays, indicating slow exchange between the double rosette assembly and its constituents on the NMR timescale.

Comparison of r_{exp} (7.3 ± 0.2 Å) and r_{calc} (9.7 Å) also suggests that assembly **SR1** is smaller than expected. The actual difference should be even larger, given the fact that assembly **SR1** is a non-spherical species (violating the conditions required for calculation of the Stokes radius).

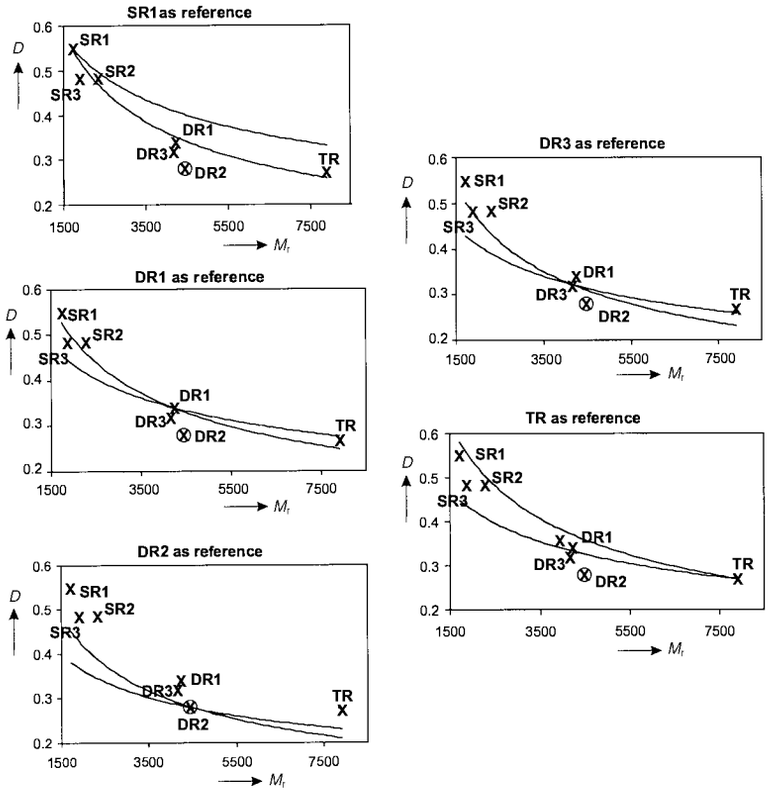

Fig. 4 Graphical analysis of D_{exp} and D_{calc} values for assemblies **SR1–3**, **DR1–3**, and **TR** with different reference assemblies (for numerical data, see Table 2). The solid lines represent the theoretical values calculated from eqn. (1). The experimental values are given by **X** and the data points for **DR2** are encircled (○).

Comparison of the diffusion coefficients for the double rosettes **DR1–DR3** and tetrarosette **TR** shows distinct differences between experimental and calculated values (both *D* and *r* values) for assembly **DR2**, while for the other assemblies these data generally show a good correlation (see Tables 1 and 2 and Fig. 4). For example, the D_{exp} value for **DR2** is far outside the range of D_{calc} values with **DR1**, **DR3**, or **TR** as a reference. Similarly, with **DR2** as reference the D_{calc} values for **DR1**, **DR3**, and **TR** are in all cases significantly lower than the D_{exp} values. The reason for the exceptional position of **DR2** is not entirely clear. **DR2** is the only double rosette assembly with isocyanurate **2b** instead of barbiturate **2a**, but this fact by itself does not explain the observed difference in the diffusion coefficients. Alternatively, the difference may originate form the fact that twelve benzyl substituents are present at the periphery of this assembly. These substituents are expected to increase the hydrolytic radii of **DR2** significantly in comparison to *e.g.* **DR1**. Assembly **DR2** lacks the six nitro groups that are present in **DR1**, but these groups are not expected to affect the hydrolytic radius much, since their position is closer to the inside of the assembly. Therefore, it seems that the relatively small M_r difference of both assemblies ($M_r = 4462$ *vs.* 4235) does not adequately reflect the difference in their effective radii and consequently the difference in their diffusion coefficients is much larger than expected from molecular weight arguments only. A similar reasoning may account for **DR3** (6 benzyl groups on the periphery), but in this case the differences are much smaller. In fact if one compares the hydrolytic radii of **DR1** and **DR3** one finds a very good agreement between r_{exp} and r_{calc}. For **DR2**, however, r_{exp} is relatively large in comparison to the other double rosettes (see Table 1).

Based on the considerations discussed, we have decided to use assembly **DR1** as a reference for the characterization of assemblies **DR4–DR6**, since **DR1** gave the best correlation between experimental and calculated diffusion data. Moreover, it has the closest structural relation (similar substituents on the periphery) to the assemblies to be characterized.

Characterization of assemblies DR4–DR6

The uniform assembly of double rosette assemblies $\mathbf{3}_3\cdot\mathbf{2}_6$ (**DR**), in which the calix[4]arene fragments are chemically fixed in the cone conformation *via* tetraalkylation at the upper rim, has been established now with more than 25 different examples.[14b] In all assemblies the calix[4]arene fragment selectively adopts one of two extreme *pinched cone* conformations, *i.e.* the one in which the aromatic rings carrying the melamine units are parallel and the remaining two rings are pointing away from each other. In order to investigate how the calix[4]arene conformation affects the thermodynamic stability of the resulting assembly, we studied the assembly behaviour of calix[4]arene dimelamines **3d** (1,3-alternate conformation, as in **DR4**), **3e** (conformationally flexible, as in **DR5**), and **4a** (alternative pinched cone conformation, as in **DR6**) by ^{1}H NMR spectroscopy, MALDI-TOF MS after Ag^+-labeling, and NMR diffusion measurements.

Synthesis of calix[4]arenes 3d, 3e, and 4a. 1,3-Alternate calix[4]arene dimelamine **3d** was prepared in 5 steps starting from dibromocalix[4]arene **6**.[19] Reaction of **6** with pentaethylene glycol ditosylate in DMF using Cs_2CO_3 as a base (and template) gave 1,3-alternate calix[4]arene **7** in 32% yield. The singlet at 3.72 ppm is highly characteristic for the methylene bridge protons of 1,3-alternate calix[4]arenes. Substitution of the bromo atoms for phthalimido† groups was performed following a slightly modified literature procedure.[20] Reaction of **7** with excess phthalimide (10 equiv.) and Cu_2O (2 equiv.) in refluxing 1-methyl-2-pyrrolidone (bp = 202 °C) for 4 days gave pure **8** in 73% yield after flash column chromatography. Removal of the phthalimide protecting groups was performed by treatment with excess hydrazine followed by conc. HCl to give diaminocalix[4]arene **9** in quantitative yield.[21] Finally, successive reaction of **9** with cyanuric chloride (3.0 equiv.) and excess gaseous ammonia gave bis(chlorotriazine) **10** in 74% yield, which was reacted without further purification with butylamine (35 equiv.)

to give calix[4]arene dimelamine **3d** in 54% yield after column chromatography. Compound **3d** has good solubility in apolar solvents like CH_2Cl_2 and $CHCl_3$.

The synthesis of the conformationally flexible tetramethoxycalix[4]arene **3e** started from 5,17-dinitrocalix[4]arene **11**,[22] which was alkylated using NaH and MeI in THF–DMF (5:1) at room temperature for 3 days to give the 5,17-dinitrocalixarene derivative **12** in 98% yield. This procedure was preferred over direct nitration of tetramethoxycalix[4]arene because of severe difficulties in isolating pure **12** from the complex mixture of nitrated products. The ^{1}H NMR spectrum of **12** at room temperature shows a complex array of signals, representing a mixture of the various conformational isomers that are present. Evidence for the clean formation of **12** was obtained by FAB-MS, which showed distinct signals at *m/z* 570.1 (100%, M^+, calc. 570.6) and 592.2 [$(M + Na)^+$, calc. 593.6]. Reduction of **12** was performed with hydrazine and Raney nickel in refluxing MeOH for 3 hours to give the corresponding diamino derivative **13** in 73% yield. Introduction of the triazine units was performed by reaction of **13** with cyanuric chloride followed by reaction with excess gaseous ammonia to give **14** in 83% yield. Finally, conversion of **14** to dimelamine **3e** was performed by refluxing with *n*-butylamine in THF in 53% yield after flash column chromatography.

Calix[4]arene diisocyanurate **4a** was prepared in two steps starting from the corresponding 5,17-bis(aminomethyl)calix[4]arene **15a** following the procedure of Whitesides and coworkers.[23] Condensation of **15a** with excess of nitrobiuret in DMF–H_2O gave the dibiuret calix[4]arene derivative **16a** in 70% yield. Treatment of **16a** with diethyl carbonate in EtOH and NaOEt as a base resulted in the precipitation of **4a** in 85% yield. Calix[4]arene diisocyanurate **4a** is scarcely soluble in chloroform and dichloromethane, but dissolves well in more polar solvents like THF, DMF, and DMSO.

Characterization and thermodynamic stability of assembly DR4

MALDI-TOF mass spectrometry. MALDI-TOF MS after Ag^+-labeling is now an established technique that has been developed in our laboratories for the MS characterization of hydrogen-bonded assemblies.[14b] So far we have successfully characterized more than 25 different **SR**, **DR**, and **TR** assemblies using this technique. The method requires the presence of a strong binding site for Ag^+ in the assembly, which acts as a cationic label to visualize the assembly under the mass spectrometric conditions. Assembly **DR4** should be able to bind Ag^+ very strongly *via* complexation inside the crown-6 ring, assisted by interaction with the π-electrons of the parallel aromatic rings of the calix[4]arene. Indeed, a sample prepared by treatment of a 1 mM chloroform solution of **3d** and **2a** (1:2 ratio) with 1.5–2.0 equiv. of $AgCF_3COO$ for 24 hours showed a very intense signal at *m/z* 4429.3 (calc. for $C_{222}H_{306}N_{48}O_{42}{\cdot}^{107}Ag^+$: 4427.1) in the MALDI-TOF MS spectrum corresponding to the monovalent Ag^+-complex of assembly **DR4** (see Fig. 5A). Other signals were not observed in the spectrum between *m/z* 2000 and 10 000 Da. In particular the intensity of the signal for **DR4**·Ag^+ indicates that assembly **DR4** is thermodynamically stable under the mass spectrometric conditions used and most likely is one of the major species present in the 1:2 mixture of **3d** and **2a**.

^{1}H NMR spectroscopy. ^{1}H NMR titration experiments of **3d** with **2a** in $CDCl_3$ gave the following results. Upon the addition of 1.0 equiv. of **2a** a new set of resonances was observed in the ^{1}H NMR spectrum at 14.4–14.0 ppm (H_a and H_b), 9.4–9.3 ppm (H_c), 8.7–8.6 ppm (H_h), and 7.8 ppm (H_d), in addition to the original signals of free **3d** (see Fig. 6A). At a 1:2 ratio of **3d** and **2a** the signals of free **3d** completely disappeared and only signals for the hydrogen-bonded assembly were observed. Further addition of **2a** did not change the spectrum, except for the appearance of a broad signal at 9.8 ppm for free **2a**. These

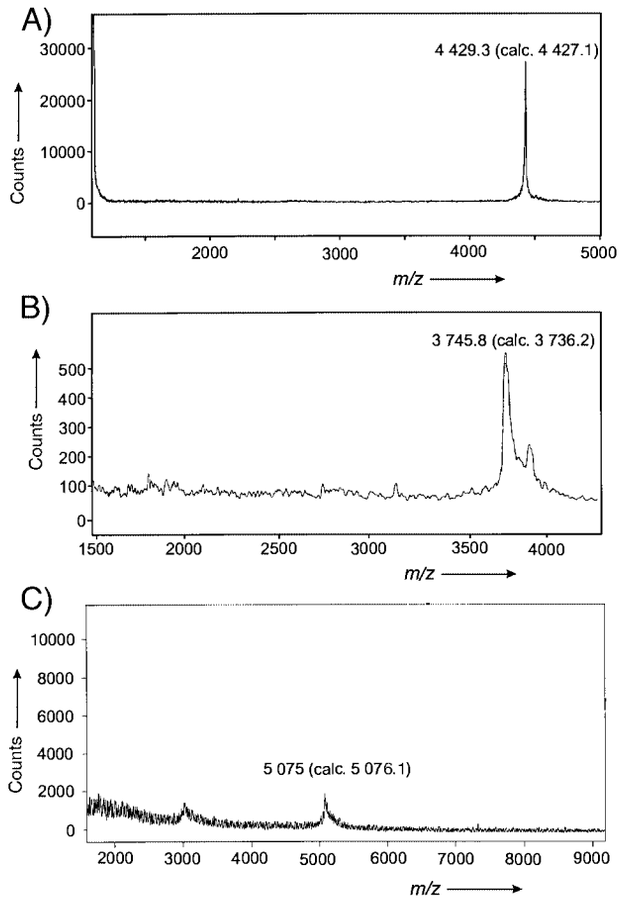

Fig. 5 MALDI-TOF MS spectra of A) 1,3-alternate calix[4]arene dimelamine **3d** and **2a** (1:2 ratio); B) flexible calix[4]arene dimelamine **3e** and **2a** (1:2 ratio); and C) pinched cone calix[4]arene **4a** and melamine **1** (1:2 ratio) after treatment with 1.5–2.0 equiv. of $AgCF_3COO$ in chloroform for 24 h at room temperature. The masses of the Ag^+-complexes of the assemblies were calculated using the chemical atomic weights of carbon, hydrogen, nitrogen, oxygen, and silver.

titration experiments clearly prove the 1:2 stoichiometry of the resulting assembly. The spectra of the titration experiments were recorded at −50 °C, because at room temperature a dynamic process was observed which made the assignment of the signals much more difficult (see Fig. 6B).

The lowfield region of the ^{1}H NMR spectrum of the 1:2 assembly at −50 °C shows four different signals for the imide $H_{a,b}$ protons (14.4–14.2 ppm) and three different signals for the H_h aromatic proton (8.7 ppm), significantly more than expected for the discrete uniform assembly **DR4**. This could be due to the presence of oligomeric assemblies or alternatively it could be caused by the presence of conformational isomers of the assembly (*i.e.* the D_3, the C_{3h} and the C_s isomers).[24] Diffusion measurements with **DR4** gave conclusive evidence of the identity of the assembly in solution. The D_{exp} of $(0.33 \pm 0.01) \times 10^{-5}$ $cm^2\ s^{-1}$ falls well within the range of D_{calc} values calculated with **DR1** as reference (see Fig. 7), which unequivocally proves the existence of the double rosette assembly **DR4** in solution. Moreover, r_{exp} (12.2 ± 0.4 Å) and r_{calc} (12.0 Å) are in very good agreement. We analyzed several different signals for each of the components of **DR4** and found practically the same diffusion coefficient for all of them. We therefore conclude that the multiple signals for the imide $H_{a,b}$ and H_h aromatic proton indicate that assembly **DR4** is present as a mixture of the three conformational isomers (*i.e.* the D_3, the C_{3h} and the C_s isomers). Determination of the relative ratio of these isomers was not possible due to insufficient resolution of the individual signals.

Comparison of the ^{1}H NMR spectra of **DR4** with that of **DR1** reveals that some of the proton signals are significantly upfield shifted. The major structural difference between these

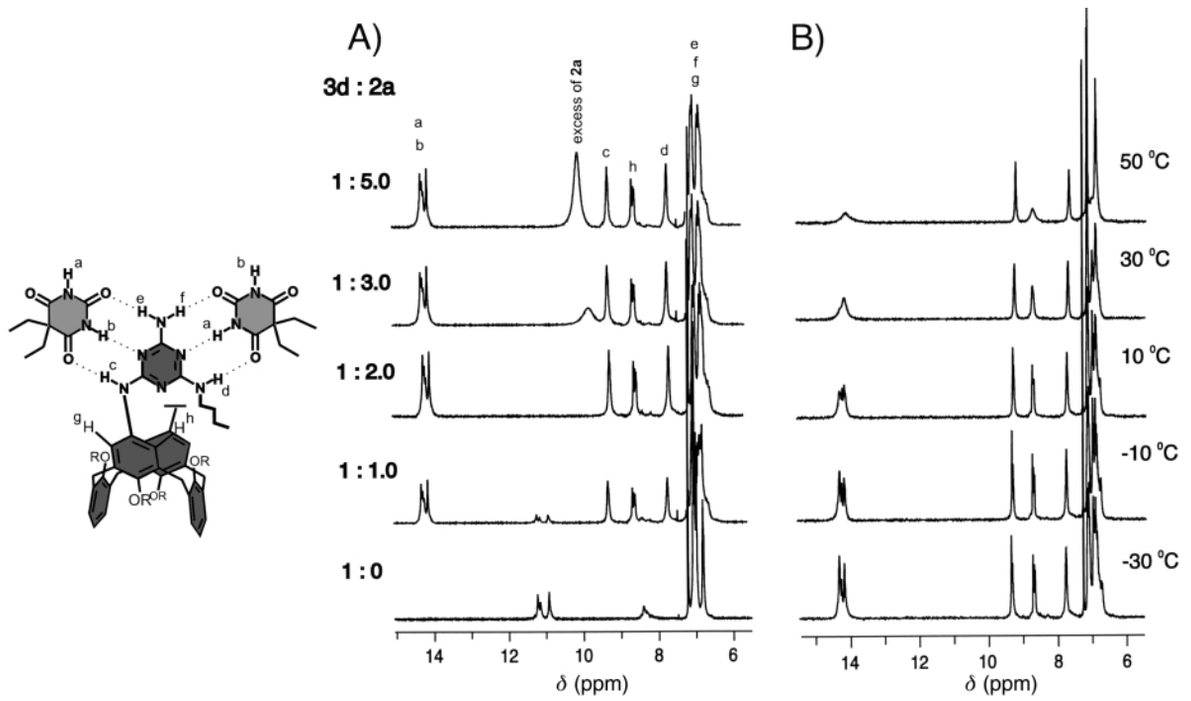

Fig. 6 A) ^{1}H NMR spectroscopic titration (400 MHz, $CDCl_3$) of 1,3-alternate calix[4]arene dimelamine **3d** and barbituric acid **2a** at −50 °C, and B) partial variable temperature ^{1}H NMR spectra of double rosette assembly **DR4**.

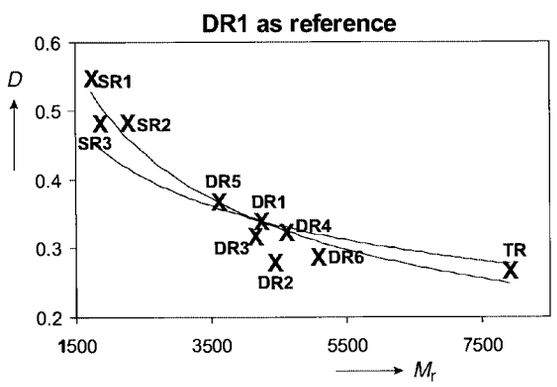

Fig. 7 Graphical analysis of D_{exp} and D_{calc} values for assemblies **DR1**–**DR6** with **DR1** as reference (for numerical data, see Table 2). The experimental values are given by **X**, whereas the solid lines represent the theoretical values calculated from eqn. (1).

assemblies is the orientation of the aromatic B and D rings of the calixarene skeleton (see Fig. 8). In **DR1** these rings are lined up as walls roughly 3.0 Å around the cyclic assembly of hydrogen bond donors and acceptors. As a consequence some of the protons are in the shielding zone of the B and D ring, which results in significant upfield shifts for these protons. In assembly **DR4** the B and D rings are positioned much more remotely from the center of the assembly and, as a consequence, some of the proton signals are significantly shifted downfield with respect to the corresponding proton signals of assembly **DR1** (for details see Table 3). First of all, protons NH_a and NH_b (hydrogen bonded C(O)NHC(O) protons) in **DR1** are observed at $\delta = 14.2$ and 13.4, whereas the same proton signals for **DR4** appear between $\delta = 14.4$ and 14.2. The difference in the upfield shift for NH_a and NH_b (~0.8 *vs.* ~0.2 ppm) is fully in agreement with the different orientation of these protons with respect to rings B and D. The effect is even more pronounced for the NH_c protons ($\Delta\delta \sim 1.0$ ppm), which seems to originate from the somewhat closer positioning of this proton with respect to ring B and D. Also the aromatic protons *ortho* to the triazine ring (H_g and H_h) undergo a similar shielding influence, with a $\Delta\delta$ of 1.7 ppm for H_h as the maximum chemical shift difference observed in assemblies **DR1** and **DR4**.

Table 3 Chemical shift differences for protons H_a–H_g in assemblies **DR1** and **DR4** (for proton assignments, see Fig. 8)

Proton	δ (ppm) in assembly **DR4**	δ (ppm) in assembly **DR1**	$\Delta\delta$ (ppm)
H_a	14.4	14.2	0.2
H_b	14.2	13.4	0.8
H_c	9.4	8.4	1.0
H_d	7.8	7.4	0.4
H_e	6.7–7.0	6.9	<0.2
H_f	6.7–7.0	6.7	<0.2
H_g	6.7–7.0	6.0	0.7–1.0
H_h	8.7	7.0	1.7

Characterization and thermodynamic stability of assembly DR5

MALDI-TOF mass spectrometry. Identification of double rosette assembly **DR5** using MALDI-TOF MS after Ag^+-labeling is questionable, since the ability to bind Ag^+ depends very strongly on the conformation that calix[4]arene **3e** adopts. However, NMR spectroscopy suggests that if assembly **DR5** exists, its component **3e** adopts a 1,3-alternate conformation, which is known to bind Ag^+ very tightly *via* cooperative interaction with the parallel aromatic rings of the calix[4]arene, forming a sandwich-type complex.[25] A sample prepared by treatment of a 1 mM chloroform solution of **3e** and **2a** (1 : 2 ratio) with 1.5–2.0 equiv. of $AgCF_3COO$ for 24 hours shows only a very weak signal at *m/z* 3745.8 (calc. for $C_{186}H_{240}N_{48}O_{30}{\cdot}^{107}Ag^+$: 3736.2) in the MALDI-TOF MS spectrum corresponding to the monovalent Ag^+-complex of **DR5** (see Fig. 5B). These data show that double rosette assembly **DR5** is present under the mass spectrometric conditions used. However, it is not possible to relate the intensity of the MALDI-TOF signal to the amount of assembly present in solution, because it strongly depends on the relative affinity of the assembly for Ag^+.

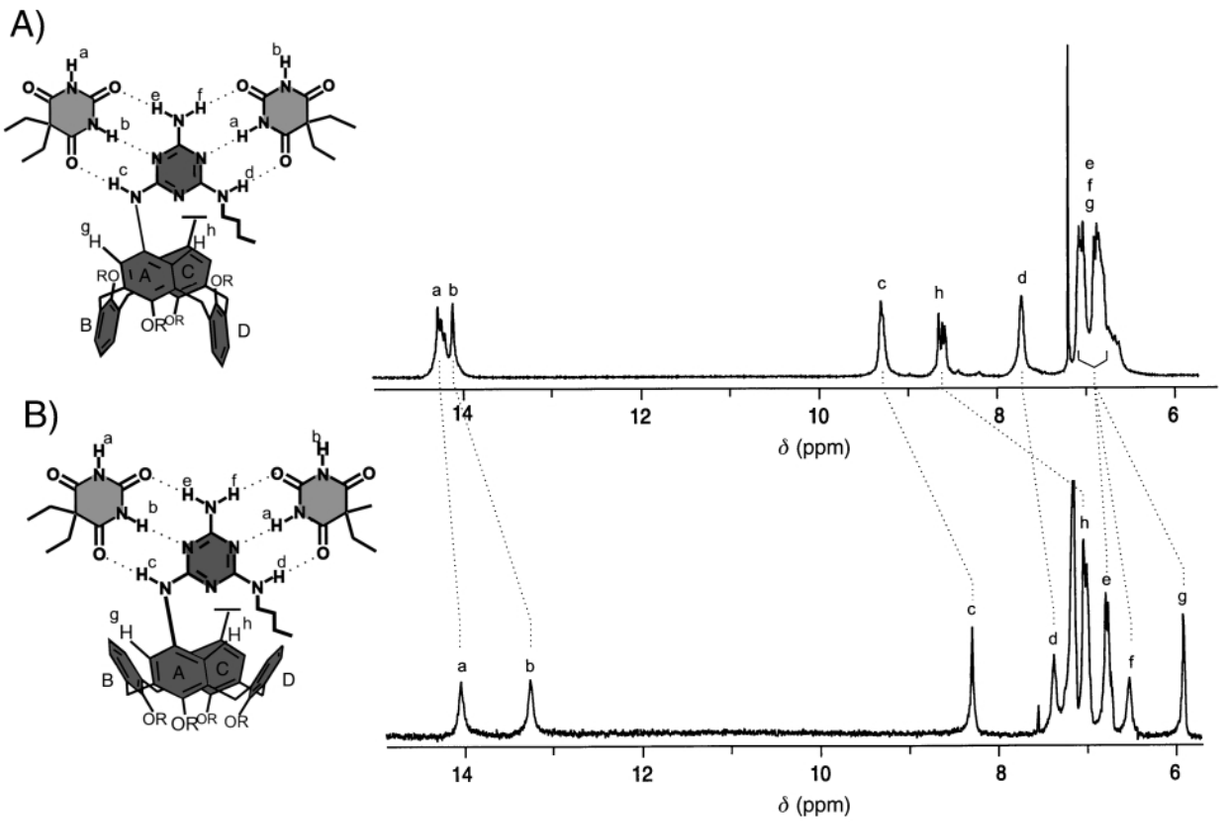

Fig. 8 Comparison of the low field part of the ^{1}H NMR spectra (300 MHz, $CDCl_3$) of A) assembly **DR4** (−50 °C) and B) assembly **DR1** (20 °C).

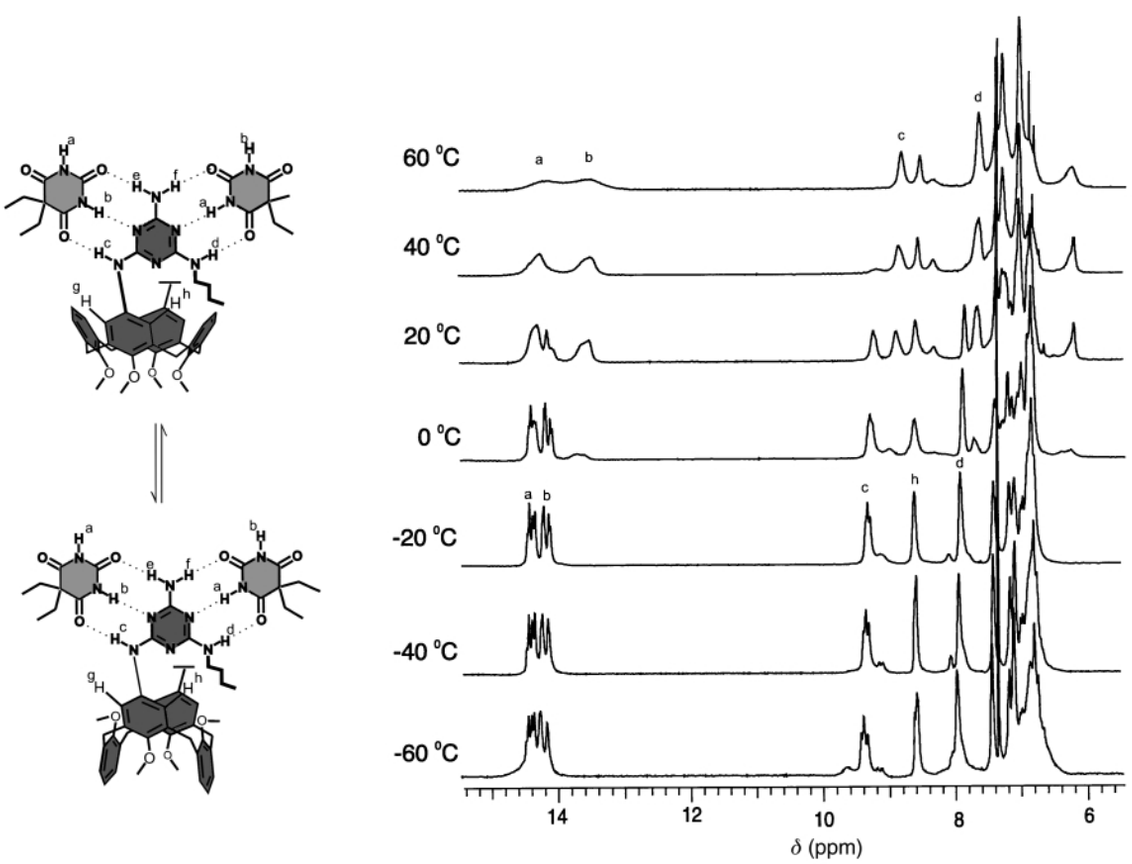

Fig. 9 Partial variable temperature ^{1}H NMR spectra (400 MHz, $CDCl_3$) of a mixture of flexible calix[4]arene dimelamine **3e** and barbituric acid **2a** (1 : 2 ratio).

^{1}H NMR spectroscopy. In the ^{1}H NMR spectrum of a 1 : 2 mixture of calix[4]arene dimelamine **3e** and barbituric acid **2a** at low temperatures (<0 °C) the position of the proton signals is very similar to those of assembly **DR4** (see Fig. 9). The proton signals for the H_a and H_b protons are observed between 14.2 and 14.5 ppm, the signals for the H_c protons around 9.4 ppm,

the signals for the H_h protons around 8.6 ppm, and the signals for the H_d protons around 8.0 ppm. However, the multitude of signals observed for each proton suggests that additional species are present in the solution. Diffusion measurements confirm this view and indicate the presence of a variety of different assemblies in the mixture. The peaks that prevailed in the PGSE spectrum were found to have very different diffusion coefficients and only one peak (3.72 ppm) had a D_{exp} of $(0.37 \pm 0.01) \times 10^{-5}$ cm^2 s^{-1}, within the range of D_{calc} values based on **DR1** as reference (see Table 1). The r_{exp} value (10.9 ± 0.3 Å) for this peak corresponds well with r_{calc} (10.7 Å), which confirms the fact that this signal corresponds to the double rosette **DR5**. Even when the diffusion measurements were repeated, the results did not change. It seems therefore that upon mixing **3e** and **2a** in a 1:2 ratio a mixture of (oligomeric) assemblies is formed, in which double rosette assembly **DR5** is only present to a minor extent. It should be noted, however, that species that give rise to broad lines in the ^{1}H NMR spectrum may escape the diffusion measurements, since their signals may be lost during the echo time of the PGSE experiments.

At higher temperatures (>0 °C) the ^{1}H NMR spectrum of **DR5** undergoes a remarkable transition. First of all an additional broad signal at around 13.5 ppm appears, while the intensity of the signals around 14.2–14.5 ppm decreases, until at 40 °C they are of equal intensity compared to the new broad signal at 13.5 ppm. In addition to this, new signals are observed at around 9.0 and 7.8–7.6 ppm. When the temperature rises above 40 °C, the original signals at 9.4 and 8.0 ppm have completely disappeared. These new signals all correspond surprisingly well with the peak positions of the hydrogen-bonded protons in double rosette assembly **DR1**, in which the calix[4]arene is fixed in the cone conformation. Apparently, the flexible calix[4]arene **3e** undergoes a conformational change from 1,3-alternate to cone between 0 and 40 °C. The reason for this conformational change is not entirely understood, but we believe that entropic factors (*e.g.* solvation) are the origin of the observed phenomenon.

The very different thermodynamic stabilities of assemblies **DR4** and **DR5** provides clear evidence that the calix[4]arene conformation plays an important role in determining the thermodynamic stability of calix[4]arene double rosette assemblies $\mathbf{3}_3\cdot\mathbf{2}_6$. The crucial difference between the flexible calix[4]arene **3e** and the rigid calix[4]arenes **3a** (cone) and **3d** (1,3-alternate) is mainly reflected in the extent of preorganization of the melamine units. Whereas the melamine units in **3e** can adopt many different relative conformations, the rigid calix[4]arene units in **3a** and **3d** fix the relative position of the melamine units to only one (U-shape), which renders the corresponding double rosette assemblies thermodynamically the most stable species in solution.

Characterization and thermodynamic stability of assembly DR6

Calix[4]arene diisocyanurate **4a** was designed to give well-defined hydrogen-bonded assemblies with large cavities inside. A methylene group separates the calix[4]arene fragment from the isocyanurate moiety, which forces these parts to be under an angle of ~120°. Molecular modelling studies suggest that calix[4]arene diisocyanurate **4a** prefers the pinched cone conformation in which the unsubstituted phenyl rings are pinched together in a parallel fashion. In this conformation three molecules of **4a** and six molecules of **1** can only form double rosette assemblies in which the individual rosettes are separated by ~10 Å thus generating an internal void. The gas phase-minimized structure (CHARMm 24.0) is shown in Fig. 3. In order to promote the formation of assembly **DR6** we used the 2,4-bis[*N*-(4-*tert*-butylphenyl)amino]-6-amino-1,3,5-triazine **1**, which has previously been shown to be unable to form tape-like assemblies as a result of steric hindrance between the bulky *tert*-butyl substituents.[27]

MALDI-TOF mass spectrometry. Identification of **DR6** with MALDI-TOF MS after Ag^+ labeling is feasible, because characterization of rosette assemblies comprising dimelamine **1** is well precedented.[14b] However, a sample of a 1:2 mixture of calix[4]arene diisocyanurate **4a** and melamine **1** showed only a very weak signal in the MALDI-TOF spectrum at *m*/*z* 5075.2 (calc. for $C_{282}H_{342}N_{54}O_{30}\cdot^{107}Ag^+$: 5076.1) after treatment with 1.5–2.0 equiv. of $AgCF_3COO$ in chloroform for 24 hours (see Fig. 5C). For pure assembly **DR6** a signal with much higher intensity would have been expected, considering the strong affinity of **1** (and most likely also **4a**) for Ag^+. Apart from a weak broad signal around *m*/*z* 3000 (corresponding to assembly fragment $[\mathbf{4a}_2\cdot\mathbf{1}_3]$, calc. *m*/*z* 3062) there is no significant signal in the spectrum up to *m*/*z* 9000. Therefore, these results indicate that (under the mass spectrometric conditions) assembly **DR6** is only present in small amounts. Most likely other (oligomeric) assemblies are formed that do not show up in the MALDI spectrum.

^{1}H NMR Spectroscopy. ^{1}H NMR titration experiments of **4a** with **1** in $CDCl_3$ gave the following results. In the presence of ≤1.0 equiv. of melamine **1** a variety of signals around 15–14 ppm (hydrogen-bonded $H_{a,b}$ protons), 11 ppm (non hydrogen-bonded $H_{a,b}$), and 10–9 ppm (hydrogen-bonded $H_{c,d}$ protons) was observed in the spectrum, the intensity being dependent on the amount of **1** present. However, when **1** was present in ≥1.5 equiv. the spectrum changed significantly. Five discrete signals around 15 ppm ($H_{a,b}$ protons, see Fig. 10A) and around 10 ppm ($H_{c,d}$ protons) were observed, whereas the signals around 11 ppm had completely disappeared. The ^{1}H NMR spectrum did not change upon the addition of more **1** (up to 8.0 equiv.) except for the appearance of additional signals (*e.g.* at 5.0 ppm) for free **1**. The spectra look similar in other solvents, such as benzene, toluene, tetrachloroethane and *o*-dichlorobenzene. In THF the hydrogen bonded assembly is no longer observed and the ^{1}H NMR spectrum exclusively displays signals for free **4a** and **1**.

It seems highly unlikely that the observed ^{1}H NMR spectra represent the clean formation of the C_{3h}-symmetrical assembly **DR6**, because the number of proton signals observed is significantly higher than expected. For example, at least seven different signals are observed for the H_a proton and five for the H_c proton (+60 °C, see Fig. 10A), while for double rosette assembly **DR6** only one single resonance is expected for each proton. Furthermore, the spectrum does not change significantly over a temperature range of −50 to +60 °C (see Fig. 10A), except for a broadening of the signals. Diffusion measurements performed on a 1:2 mixture of **4a** and **1** in chloroform gave a D_{exp} of $(0.29 \pm 0.01) \times 10^{-5}$ cm^2 s^{-1}, a value that is slightly lower than the range of the D_{calc} values $[(0.31 \pm 0.01) \times 10^{-5}$ cm^2 s^{-1} < D < $(0.32 \pm 0.01) \times 10^{-5}$ cm^2 s$^{-1}]$ for assembly **DR6** (M_r 4966). Also r_{exp} (13.9 ± 0.5 Å) is larger than calculated from molecular modeling (13.0 Å). These data suggest that double rosette assembly **DR6** is thermodynamically less stable and that significant amounts of different other species prevail in the solution. It should be noted that for this double rosette only a few signals could be analyzed since others were too broad to be analyzed. Therefore the existence of other species in this solution also seems plausible based on the diffusion measurements.

In a related study on the spontaneous assembly of hydrogen-bonded rod-like polymers $[\mathbf{4}_3\cdot\mathbf{3}_3]_n$ it was found that assembly of the lipophilic calix[4]arene dimelamine **3f** ($R^1 = C_{12}H_{25}$) with calix[4]arene diisocyanurate **4b** ($R^1 = C_{12}H_{25}$) (1:1 ratio) resulted in the formation of very well-defined rod-like polymer structures, from which the ^{1}H NMR spectra indicate the exclusive formation of the corresponding cyclic double rosette structure (see Fig. 10B).[9] These results seem to suggest that the apparent steric repulsion between the *tert*-butyl substituents

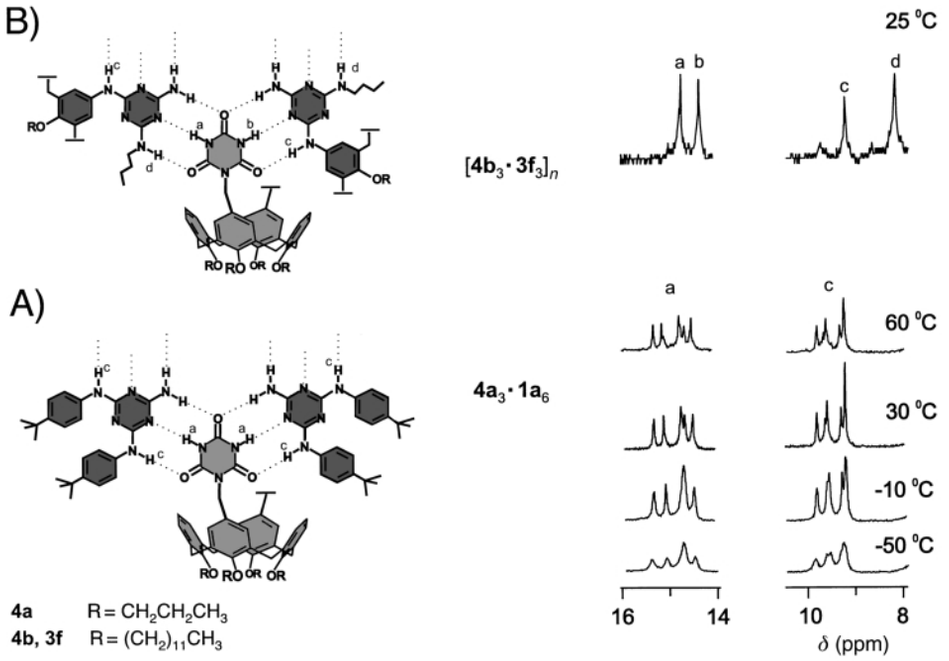

Fig. 10 A) Partial variable temperature ^{1}H NMR spectra (400 MHz, $CDCl_3$) of a mixture of calix[4]arene biscyanurate **4a** and melamine **1** (1 : 2 ratio) in $CDCl_3$; B) ^{1}H NMR spectrum of a mixture of calix[4]arene biscyanurate **4b** and calix[4]arene dimelamine **3f** (1 : 1 ratio) at 25 °C in toluene-d_8.

of neighbouring melamine units **1** in the corresponding tape-like assemblies seems insufficient to direct the clean formation of double rosette assembly **DR6**, resulting in the concomitant formation of significant amounts of ill-defined higher order assemblies. A more detailed discussion about the role of steric interactions in determining tape *vs.* rosette formation will be described elsewhere.

Conclusions

NMR diffusion spectroscopy provides a useful technique that can assist in the characterization of hydrogen-bonded assemblies in solution. The technique has sufficient resolution to distinguish between single, double and tetrarosette assemblies. It has been successfully applied to the characterization of a number of assemblies from which the characterization by other methods was so far not clear. Our results clearly show that the calix[4]arene conformation of dimelamines **3** significantly affects the thermodynamic stability of the corresponding double rosette assemblies. Calix[4]arenes fixed in a *pinched cone* conformation (**DR1–3**) or a *1,3-alternate* conformation (**DR4**) provide sufficient preorganization of the melamine units to promote exclusive formation of the corresponding double rosette assemblies. In contrast to this, the thermodynamic stability for double rosette assemblies based on flexible calix[4]arenes is significantly lower because flexible calix[4]arene units do not provide sufficient preorganization. In this case, significant amounts of other (oligomeric) assemblies are formed. Similarly, the pinched conformation in calix[4]arenes **4a** cannot stabilize double rosette structures in the absence of dimelamines **3** and therefore mainly polymeric assemblies are observed in the presence of melamine **1**.

Experimental

Synthesis

All synthetic experiments were carried out in an argon atmosphere. THF was distilled from Na–benzophenone ketyl, petroleum ether (bp 60–80 °C), CH_2Cl_2 from K_2CO_3. All chemicals were of reagent grade and used without further purification. Melting points were determined with a Reichert melting point apparatus and are uncorrected. Flash chromatography was performed on silica gel (SiO_2, E. Merck, 0,040–0.063 mm, 230–240 mesh). The presence of solvents in the analytical samples was confirmed by ^{1}H NMR spectroscopy. Experimental procedures for the synthesis of melamine derivatives **1**,[26] isocyanuric acid derivative **2b**,[24] calix[4]arene dimelamines **3a–c**,[14d,24] tetramelamine **5**,[15] calix[4]arene derivatives **6**,[19] **11**,[22] and **15**[28] have been or will be described elsewhere.

NMR spectroscopy

NMR spectra were recorded on a Bruker AC250 (^{1}H NMR 250 MHz) or a Varian Unity 400 (^{1}H NMR 400 MHz) spectrometer in $CDCl_3$ at room temperature unless stated otherwise. Residual solvent protons were used as internal standard and chemical shifts are given relative to tetramethylsilane (TMS). *J* values are given in Hertz. Diffusion experiments were carried out on a 500 MHz ARX Bruker (Karlshrue, Germany) NMR spectrometer equipped with a B-VT-2000 temperature unit and a B-AFPA10 pulsed gradient unit capable of producing magnetic field pulse gradients in the *z*-direction of about 50 G cm^{-1}. All experiments were carried out in a 5 mm inverse probe at 298 K. The $CDCl_3$ solution of the compound (2 mM) was placed in a 4 mm NMR tube that was inserted into a 5 mm NMR tube (Willmad, USA) to avoid sample heating during the magnetic field pulse gradients. The magnetic field pulse gradients were of 2 ms duration, and their separation was 62 ms. The pulse gradients were incremented from 0 to 46.8 G cm^{-1} in ten steps. In all experiments at least two peaks, each from different components of the rosette, were analyzed. The diffusion experiments were preformed at least three times and only data for which the correlation coefficient (*R*) was higher than 0.999 were included.

Mass spectrometry

Fast atom bombardment (FAB) and electron impact (EI) spectra were measured on a Finnigan MAT 90 spectrometer with *m*-nitrobenzyl alcohol (NBA) as a matrix. Matrix assisted laser desorption ionization (MALDI) time-of-flight (TOF) mass spectrometry measurements were performed on a PerSeptive

Biosystems Voyager-DE-RP spectrometer (PerSeptive Biosystems, Inc., Framingham, MA, USA) equipped with delayed extraction. A 337 nm UV nitrogen laser producing 3 ns pulses was used in the linear and reflectron mode. Samples for Ag^+-labeling experiments were prepared by stirring 5–10 mM solutions of the hydrogen-bonded assemblies in $CHCl_3$ with 1.5 equiv. (per mol assembly) of solid $AgCF_3COO$ (Acros, 98% purity) for 24 h and mixing 10 μL of this solution with 30 μL of a solution of 3 mg L^{-1} 2,5-dihydroxybenzoic acid (DHB) in $CHCl_3$. 1 μL of the resulting solution was loaded on a gold sample plate, the solvent was removed in warm air and the sample transferred to the vacuum of the mass spectrometer for analysis.

5,17-Dibromo-25,27-dipropoxy-26,28-(3,6,9,12-tetraoxatetradecane-1,14-diyldioxy)calix[4]arene, 1,3-alternate (7). A mixture of calix[4]arene derivative **6** (100 mg, 0.15 mmol) and Cs_2CO_3 (733 mg, 2.25 mmol) in DMF (25 mL) was heated at 80 °C for 15 min. Subsequently, pentaethylene glycol ditoluene-*p*-sulfonate (90 mg, 0.165 mmol) was added and the reaction mixture was heated at 80 °C for 16 h. Then DMF was removed under reduced pressure and the residue was dissolved in CH_2Cl_2 (25 mL), washed with H_2O (2 × 25 mL), and dried over Na_2SO_4. Evaporation of the solvent gave a brown solid material, which was purified by column chromatography (SiO_2, 1% MeOH–CH_2Cl_2) to give pure 1,3-alternate calix[4]arene **7** as a white solid (42 mg, 32%). Mp 180–185 °C. ^{1}H NMR δ_H = 7.18 (4H, s, *o*-BrArH), 7.08 (4H, d, *J* 7.3, *m*-OPrArH), 6.84 (2H, t, *p*-OPrArH), 3.72 (8H, s, $ArCH_2Ar$), 3.70 (4H, s, OCH_2), 3.7–3.6 (4H, m, $OCH_2CH_2CH_3$), 3.6–3.5 (8H, m, OCH_2), 3.5–3.4 (8H, m, OCH_2), 1.43 (4H, m, OCH_2), 0.88 (6H, t, *J* 7.5, CH_3). ^{13}C NMR δ_C = 156.6, 155.3, 135.8, 133.3, 132.3, 129.8, 122.3, 114.7, 72.0, 71.1, 70.9, 70.3, 69.8, 37.3, 22.5, 10.1. MS (FAB) *m*/*z* 868.8 [100%, $(M + H)^+$].

5,17-Diphthalimido-25,27-dipropoxy-26,28-(3,6,9,12-tetraoxatetradecane-1,14-diyldioxy)calix[4]arene, 1,3-alternate (8). A suspension of calix[4]arene derivative **7** (458 mg, 0.527 mmol), phthalimide (776 mg, 5.27 mmol) and Cu_2O (158 mg, 1.107 mmol) in 1-methyl-2-pyrrolidone (10 mL) was refluxed for 4 d. The reaction mixture was cooled to room temperature, H_2O (200 mL) was added and the resulting suspension was filtered and the black solid was dissolved in CH_2Cl_2 (25 mL). In order to remove residual H_2O, dry toluene (10 mL) was added and the solution was concentrated to dryness under reduced pressure. This was repeated twice then the black residue was further dried *in vacuo* for 1 h and purified by column chromatography (SiO_2, 3% MeOH–CH_2Cl_2) to give diphthalimide **8** as a slightly yellow solid (385 mg, 73%). Mp 293–295 °C. ^{1}H NMR δ_H = 7.9–7.8 (4H, m, ArH(phthalimide)), 7.8–7.7 (4H, m, ArH(phthalimide)), 7.18 (4H, s, *o*-phthalimidoArH), 7.11 (4H, d, *J* 7.6, *m*-OPrArH), 6.86 (2H, t, *J* 7.5, *p*-OPrArH), 3.87 (8H, s, $ArCH_2Ar$), 3.72 (4H, s, OCH_2), 3.7–3.6 (8H, m, OCH_2), 3.6–3.5 (4H, m, OCH_2), 3.48 (4H, t, *J* 7.5, $OCH_2CH_2CH_3$), 3.22 (4H, t, *J* 6.4, OCH_2), 1.38 (4H, m, $OCH_2CH_2CH_3$), 0.65 (6H, t, *J* 7.5, $OCH_2CH_2CH_3$). ^{13}C NMR δ_C = 167.2, 157.1, 155.9, 134.1, 134.0, 133.2, 131.8, 129.4, 126.8, 126.0, 123.4, 122.0, 72.7, 71.1, 70.8, 70.5, 69.4, 69.0, 37.9, 22.7, 10.0. MS (FAB) *m*/*z* 1000.7 [100%, $(M + H)^+$].

5,17-Diamino-25,27-dipropoxy-26,28-(3,6,9,12-tetraoxatetradecane-1,14-diyldioxy)calix[4]arene, 1,3-alternate (9). To a solution of calix[4]arene derivative **8** (1.077 g, 1.076 mmol) in EtOH (50 mL) hydrazine hydrate (0.31 mL, 6.45 mmol) was added and the solution was refluxed for 2 h, followed by treatment with concentrated HCl (2 mL, 12 M) for 30 min. The solution was evaporated to dryness, the residue taken up in CH_2Cl_2, subsequently washed with 2 M NaOH, H_2O till neutrality, and dried over Na_2SO_4. The solution was filtered and evaporated to dryness to give pure diaminocalix[4]arene **9** as a yellow–orange solid (0.76 g, 96%). Mp 112–115 °C. ^{1}H NMR δ_H = 7.06 (4H, d, *J* 7.3, *m*-OPrArH), 6.81 (2H, t, *J* 7.5, *p*-OPrArH), 6.41 (4H, s, *o*-NH_2ArH), 3.71 (8H, s, $ArCH_2Ar$), 3.7–3.6 (8H, m, OCH_2 + $OCH_2CH_2CH_3$), 3.6–3.4 (8H, m, OCH_2), 3.4–3.3 (8H, m, OCH_2), 3.0 (4H, br s, NH_2), 1.44 (4H, m, $OCH_2CH_2CH_3$), 0.81 (6H, t, *J* 7.5, $OCH_2CH_2CH_3$). ^{13}C NMR δ_C = 156.7, 149.4, 140.5, 134.4, 134.0, 129.7, 122.0, 117.0, 72.3, 71.1, 70.9, 70.0, 69.8, 37.9, 22.8, 10.2. MS (FAB) *m*/*z* 740.3 [100%, $(M + H)^+$]. Found: C, 70.7; N, 3.7; H, 7.55. Calc. for $C_{44}H_{56}N_2O_8 \cdot 0.5H_2O$: C, 70.5; N, 3.7; H, 7.7%.

5,17-Bis(4-amino-6-chloro-1,3,5-triazin-2-ylamino)-25,27-dipropoxy-26,28-(3,6,9,12-tetraoxatetradecane-1,14-diyldioxy)-calix[4]arene, 1,3-alternate (10). To an ice-cold solution of cyanuric chloride (224 mg, 1.215 mmol) and diisopropylethylamine (0.42 mL, 2.43 mmol) in dry THF (10 mL), calix[4]arene derivative **9** (300 mg, 0.405 mmol) was added in small portions at 0 °C. After stirring the mixture for 3 h at 0 °C gaseous ammonia was gently bubbled through the solution for another 3 h, while keeping the temperature at 0 °C. The reaction mixture was concentrated to dryness *in vacuo* at ambient temperature. The residue was taken up in CH_2Cl_2–H_2O (200 : 100 mL). After separation of the layers the aqueous layer was extracted with CH_2Cl_2 (2 × 50 mL) and the combined organic layers were washed with H_2O (2 × 100 mL), and dried over Na_2SO_4. Evaporation of the solvent gave crude bis(chlorotriazine) **10** (300 mg, 74%), which was used without further purification. ^{1}H NMR (DMSO-d_6) δ_H = 9.7 (2H, br s, ArNH), 7.04 (4H, d, *J* 7.3, *m*-OPrArH), 6.75 (2H, t, *J* 7.3, *p*-OPrArH), 5.76 (4H, s, *o*-NHArH), 3.7 (8H, br s, $ArCH_2Ar$), 3.57 (4H, s, OCH_2), 3.6–3.5 (4H, m, $OCH_2CH_2CH_3$), 3.5–3.3 (8H, m, OCH_2), 3.3–3.0 (8H, m, OCH_2), 1.3–1.1 (4H, m, $OCH_2CH_2CH_3$), 0.54 (6H, t, *J* 7.3, $OCH_2CH_2CH_3$). MS (FAB) *m*/*z* 997.3 [100%, $(M + H)^+$].

5,17-Bis[4-amino-6-(butylamino)-1,3,5-triazin-2-ylamino]-25,27-dipropoxy-26,28-(3,6,9,12-tetraoxatetradecane-1,14-diyldioxy)calix[4]arene-crown-6, 1,3-alternate (3d). A solution of bis(chlorotriazine) **10** (300 mg, 0.30 mmol), diisopropylethylamine (0.63 mL, 3.6 mmol), and *n*-butylamine (1.04 mL, 10.5 mmol) in dry THF (100 mL) was refluxed for 18 h and subsequently concentrated to dryness. The residue was taken up in CH_2Cl_2–H_2O (100 : 50 mL) and after separation the organic layer was washed with brine (100 mL), water (2 × 100 mL), and dried over Na_2SO_4. Evaporation of the solvent gave crude calix[4]arene dimelamine **3d**, which was purified by column chromatography (SiO_2, 2% MeOH–CH_2Cl_2) to give pure **3d** as a glassy solid (177 mg, 54%). Mp 148–150 °C. ^{1}H NMR δ_H = 7.2–7.0 (8H, m, *o*-NHArH + *m*-OPrArH), 6.83 (2H, t, *J* 7.3, *p*-OPrArH), 3.9–3.6 (20H, m, $ArCH_2Ar$ + OCH_2), 3.6–3.4 (12H, m, $OCH_2CH_2CH_3$ + OCH_2), 3.4–3.2 (4H, m, $NHCH_2$), 1.6–1.4 (8H, m, $NHCH_2(CH_2)_2CH_3$), 1.4–1.2 (4H, m, OCH_2-CH_2CH_3), 0.89 (6H, t, *J* 7.2, $NH(CH_2)_3CH_3$), 0.69 (6H, t, *J* 7.3, $OCH_2CH_2CH_3$). MS (FAB) *m*/*z* 1071.5 [100%, $(M + H)^+$].

5,17-Dinitro-25,26,27,28-tetramethoxycalix[4]arene (12). To a solution of dinitrocalix[4]arene **11** (200 mg, 0.369 mmol) in THF–DMF (10 : 2 mL) were added NaH (60% in oil, 221 mg, 5.53 mmol) and MeI (0.34 mL, 5.53 mmol) under Ar. The reaction mixture was stirred at room temperature for 3 d. Water (1 mL) was added and the solution was evaporated to dryness. The residue was taken up in CH_2Cl_2–H_2O (100 : 50 mL) and after separation the organic layer was washed with water (2 × 50 mL), and dried over Na_2SO_4. The solution was filtered and evaporated to dryness to give crude **7**, which was purified by column chromotography (SiO_2, CH_2Cl_2) to give pure **12** as a slightly yellow solid (206 mg, 98%). Mp 261–263 °C. ^{1}H NMR

δ_H = 8.3–6.2 (10H, m, ArH), 4.4–2.8 (20H, m, $ArCH_2Ar$ + OCH_3). MS (FAB) *m/z* 570.1 [100%, $(M + H)^+$].

5,17-Diamino-25,26,27,28-tetramethoxycalix[4]arene (13). Hydrazine hydrate (2.6 mL, 52.6 mmol) was added dropwise to a suspension of dinitrocalix[4]arene **12** (1.00 g, 1.75 mmol) and a catalytic amount of Raney Ni in MeOH (120 mL). After 3 h reflux under argon, the Raney Ni was filtered over Hyflo and the solvent was evaporated. The residue was taken up in CH_2Cl_2 (100 mL) and washed with water. After drying over Na_2SO_4, evaporation of the solvent gave crude diaminocalix[4]arene **13** as an orange–brown solid (650 mg, 73%), which was used without further purification. Mp 245–250 °C (slow phase transition). ^{1}H NMR δ_H = 7.2–5.8 (10H, m, ArH), 4.4–2.5 (24H, m, $ArCH_2Ar$ + OCH_3 + NH_2). MS (FAB) *m/z* 510.3 [100%, $(M + H)^+$.

5,17-Bis(4-amino-6-chloro-1,3,5-triazin-2-ylamino)-25,26,27,28-tetramethoxycalix[4]arene (14). To an ice-cold solution of cyanuric chloride (704 mg, 3.82 mmol) and diisopropylethylamine (1.33 mL, 7.64 mmol) in dry THF (30 mL), diaminocalix[4]arene **13** (650 mg, 1.27 mmol) was added in small portions at 0 °C. After stirring the mixture for 3 h at 0 °C gaseous ammonia was gently bubbled through the solution for another 3 h, while keeping the temperature at 0 °C. The reaction mixture was concentrated to dryness *in vacuo* at ambient temperature. The residue was taken up in CH_2Cl_2–H_2O (500 : 200 mL). After separation of the layers the aqueous layer was extracted with CH_2Cl_2 (2 × 100 mL) and the combined organic layers were washed with H_2O (2 × 200 mL), and dried over Na_2SO_4. Evaporation of the solvent gave crude bis(chlorotriazine) **14** (800 mg, 82%), which was used without further purification. ^{1}H NMR (DMSO-d_6) δ_H = 7.6–6.2 (10H, m, ArH), 4.4–2.8 (20H, m, $ArCH_2Ar$ + OCH_3). MS (FAB) *m/z* 767.3 [100%, $(M + H)^+$].

5,17-Bis[4-amino-6-(butylamino)-1,3,5-triazin-2-ylamino]-25,26,27,28-tetramethoxycalix[4]arene (3e). A solution of bis(chlorotriazine) **14** (800 mg, 1.04 mmol), diisopropylethylamine (1.82 mL, 10.4 mmol), and *n*-butylamine (2.06 mL, 20.8 mmol) in dry THF (150 mL) was refluxed for 22 h and subsequently concentrated to dryness. The residue was taken up in CH_2Cl_2–H_2O (200 : 100 mL) and after separation the organic layer was washed with brine (100 mL), water (2 × 100 mL), and dried over Na_2SO_4. Evaporation of the solvent gave crude calix[4]arene dimelamine **3e**, which was purified by column chromatography (SiO_2, 3% MeOH–CH_2Cl_2) to give pure **3e** as a slightly brown solid (465 mg, 53%). Mp 182–185 °C. ^{1}H NMR δ_H = 7.3–6.2 (10H, m, ArH), 4.4–2.7 (24H, m, $ArCH_2Ar$ + OCH_3 + $NHCH_2$), 1.7–1.2 (8H, m, $NHCH_2(CH_2)_2CH_3$), 0.92 (6H, t, *J* 7.0, $NH(CH_2)_3CH_3$). MS (FAB) *m/z* 841.9 [100%, $(M + H)^+$]. Found: C, 64.7; N, 19.6; H 6.8. Calc. for $C_{46}H_{56}N_{12}O_4 \cdot 0.75H_2O$: C, 64.7; N, 19.7; H, 6.8%.

5,17-Bis(amidoureidomethyl)-25,26,27,28-tetrapropoxycalix[4]arene (16a). To a solution of bis(methylamino)calix[4]arene **15a** (1.5 g, 2.3 mmol) in DMF (70 mL) and H_2O (15 mL) were added nitrobiuret (1.0 g, 6.8 mmol) and Na_2HPO_4 (2.0 g, 14.1 mmol). The resulting mixture was heated under an argon atmosphere at 95 °C for 1 h, then a further 1.0 g of nitrobiuret was added and the heating was continued. After 1 h, a third portion of nitrobiuret (1.0 g, 6.8 mmol) was added and heating continued for 1.5 h. The mixture was cooled to room temperature and the solvent was removed under reduced pressure. The residue was dissolved in CH_2Cl_2 (200 mL) and this solution was washed with HCl (1 M, 2 × 100 mL), water (2 × 100 mL) and brine (100 mL) then dried ($MgSO_4$) and the solvent was removed under reduced pressure to yield a yellow oil. Trituration with methanol (30 mL) gave bis(biuret)calix[4]arene **16a** as a colorless solid (1.3 g, 70%). Mp 267–269 °C. ^{1}H NMR (250 MHz, DMSO-d_6) δ_H = 8.62 (2H, s, NH), 7.75 (2H, br s, NH), 6.82 (8H, s, ArH), 6.3 (6H, m, ArH), 4.32 and 3.13 (8H, ABq, *J* 15.7, $ArCH_2Ar$), 4.12 (4H, d, *J* 7, NCH_2), 3.88 (4H, t, *J* 8.1, $OCH_2CH_2CH_3$), 3.67 (4H, t, *J* 8.1, $OCH_2CH_2CH_3$), 2.0–1.8 (8H, m, $OCH_2CH_2CH_3$), 1.03 (6H, t, *J* 8.8, $OCH_2CH_2CH_3$), 0.91 (6H, t, *J* 8.9, $OCH_2CH_2CH_3$). MS (FAB) *m/z* 845 [100%, $(M + Na)^+$]. Found: C, 66.8; H, 7.0; N, 9.7. Calc. for $C_{46}H_{58}N_6O_8 \cdot 0.5H_2O$: C, 66.4; H, 7.2; N, 10.1%.

5,17-Bis(2,4,6-trioxoperhydro-1,3,5-triazinylmethyl)-25,26,27,28-tetrapropoxycalix[4]arene (4a). To a solution of sodium ethoxide generated *in situ* from Na (0.25 g, 10.9 mmol) and ethanol (50 mL) under an argon atmosphere were added compound **16a** (0.65 g, 0.8 mmol) and diethyl carbonate (0.52 mL, 4.3 mmol). The mixture was heated at reflux for 24 h, then cooled to room temperature and water (10 mL) was added followed by HCl (6 M) until the solution reached pH 1. The acidified solution was extracted with ethyl acetate (3 × 75 mL) and the organic solutions were combined and washed with water (100 mL) and brine (100 mL), then dried ($MgSO_4$). The solvent was removed under reduced pressure to give a white solid which was purified by column chromatography (silica; $CHCl_3$–MeOH; 9 : 1) to yield compound **4a** (0.6 g, 87%). Mp > 300 °C. ^{1}H NMR (250 MHz, DMSO-d_6) δ_H = 11.71 (4H, s, NH), 6.9 (4H, m, ArH), 6.2–6.3 (6H, m, ArH), 4.70 (4H, s, NCH_2), 4.29 and 3.13 (8H, ABq, *J* 15.7, $ArCH_2Ar$), 3.6 (4H, m, $OCH_2CH_2CH_3$), 3.9 (4H, m, $OCH_2CH_2CH_3$), 1.75–1.95 (8H, m, $OCH_2CH_2CH_3$), 1.03 (6H, t, *J* 8.8, $OCH_2CH_2CH_3$), 0.88 (6H, t, *J* 8.8, $OCH_2CH_2CH_3$). MS (FAB) *m/z* 873 [100%, $(M - H)^+$]. Found: C, 65.3; H, 6.5; N, 9.1. Calc. for $C_{48}H_{54}N_6O_{10} \cdot 0.5H_2O$: C, 65.2; H, 6.3; N, 9.5%.

Assembly formation. Assemblies **SR1–3**, **DR1–DR5**, and **TR** are typically formed by mixing the melamine and the barbituric acid/isocyanuric acid components in chloroform, followed by stirring the resulting suspension at room temperature until homogeneous (1 h). After evaporation of the solvent rosettes are obtained as glassy solids in quantitative yield.

For assembly **DR6** a different procedure was used because of the low solubility of **4a** in chloroform. The individual components were first dissolved in THF, then mixed together and after evaporation of the solvent a chloroform-soluble residue was obtained.

Molecular mechanics calculations

Initial structures, created by manual modifications of the X-ray crystal structure of **DR1**,[14d] as well as visualizations were carried out with Quanta 97.[29] All gas phase simulations were performed with CHARMm version 24.0[30] as implemented in Quanta 97. Parameters were taken from Quanta 97 and point charges were assigned with the charge-template option. Residual charge was smoothed on carbon and non-polar hydrogen atoms rendering overall neutral residues. A distance-dependent relative permittivity was applied with $\varepsilon = 1$. No cut-offs on the non-bonded interactions were used. Energy minimizations were performed with the steepest descent and adopted basis Newton–Raphson methods until the root mean square of the energy gradient was < 0.001 kcal mol^{-1} $Å^{-1}$.

Acknowledgements

We are grateful to Dr R. Hulst for performing the VT and 2D NMR experiments and to Professor N. Nibbering and R. Fokkens (Institute of Mass Spectrometry, University of Amsterdam) for the MALDI-TOF measurements. Furthermore, we thank JST (Chemotransfiguration Project) for financial support to Dr K. A. Jolliffe and NWO/CW for financial support to Dr L. J. Prins.

References

1 G. M. Whitesides, E. E. Simanek, J. P. Mathias, C. T. Seto, D. N. Chin, M. Mammen and D. M. Gorden, *Acc. Chem. Res.*, 1995, **28**, 37.

2 S. J. Geib, C. Vincent, E. Fan and A. D. Hamilton, *Angew. Chem., Int. Ed. Engl.*, 1993, **32**, 119.

3 M. R. Ghadiri, J. R. Granja, R. A. Milligan, D. E. McRee and N. Khazanovich, *Nature*, 1993, **366**, 324.

4 (*a*) T. Heinz, D. M. Rudkevich and J. Rebek, Jr., *Nature*, 1998, **394**, 764; (*b*) T. Martin, U. Obst and J. Rebek, Jr., *Science*, 1998, **281**, 1842; (*c*) R. Meissner, J. Rebek, Jr. and J. de Mendoza, *Science*, 1995, **270**, 1485.

5 J. L. Atwood and L. R. MacGillivray, *Nature*, 1997, **389**, 469.

6 O. Mogck, M. Pons, V. Bohmer and W. Vogt, *J. Am. Chem. Soc.*, 1997, **119**, 5706.

7 S. C. Zimmerman, F. Zeng, D. E. C. Reichert and S. V. Kolotuchin, *Science*, 1996, **271**, 1095.

8 R. P. Sijbesma, F. H. Beijer, L. Brunsveld, B. J. B. Folmer, J. H. K. K. Hirschberg, R. F. M. Lange, J. K. L. Lowe and E. W. Meijer, *Science*, 1997, **278**, 1601.

9 H.-A. Klok, K. A. Jolliffe, C. L. Schauer, J. P. Spatz, M. Moller, P. Timmerman and D. N. Reinhoudt, *J. Am. Chem. Soc.*, 1999, **121**, 7154.

10 P. Lipkowski, A. Bielejewska, H. Kooijman, A. L. Spek, P. Timmerman and D. N. Reinhoudt, *Chem. Commun.*, 1999, 1311.

11 E. O. Stejskal and J. E. Tanner, *J. Chem. Phys.*, 1965, **42**, 288. For a review concerning the applications of the PGSE NMR technique to chemical systems see: P. Stilbs, *Prog. Nucl. Magn. Reson. Spectrosc.*, 1987, **19**, 1, and references cited therein.

12 (*a*) O. Mayzel and Y. Cohen, *J. Chem. Soc., Chem. Commun.*, 1994, 1901; (*b*) O. Mayzel, O. Aleksiuk, F. Grynszpan, S. E. Biali and Y. Cohen, *J. Chem. Soc., Chem. Commun.*, 1995, 1183; (*c*) O. Mayzel, A. Gafni and Y. Cohen, *Chem. Commun.*, 1996, 911; (*d*) A. Gafni and Y. Cohen, *J. Org. Chem.*, 1997, **62**, 120; (*e*) A. Gafni, Y. Cohen, R. Kataky, S. Palmer and D. Parker, *J. Chem. Soc., Perkin Trans. 2*, 1998, 19; (*f*) L. Frish, S. E. Matthews, V. Böhmer and Y. Cohen, *J. Chem. Soc., Perkin Trans. 2*, 1999, 669; (*g*) B. Olenyuk, M. D. Levin, J. A. Whiteford, J. E. Shield and P. J. Stang, *J. Am. Chem. Soc.*, 1999, **121**, 10434; (*h*) A. C. S. Lino and W. Loh, *J. Inclusion Phenom. Macrocyclic Chem.*, 2000, **36**, 267; (*i*) P. J. Skinner, S. Blair, R. Kataky and D. Parker, *New J. Chem.*, 2000, **24**, 265.

13 (*a*) K. F. Morris and C. S. Johnson, Jr., *J. Am. Chem. Soc.*, 1992, **114**, 776; (*b*) K. F. Morris and C. S. Johnson, Jr., *J. Am. Chem. Soc.*, 1992, **114**, 3139; (*c*) C. S. Johnson, Jr., *Prog. Nucl. Magn. Reson. Spectrosc.*, 1999, **34**, 203 and references cited therein; (*d*) M. D. Pelta, H. Barjat, G. A. Morris, A. L. Davis and S. J. Hammond, *Magn. Reson. Chem.* 1998, **36**, 706; (*e*) H. Barjat, G. A. Morris and A. G. Swanson, *J. Magn. Reson.*, 1998, **131**, 131.

14 (*a*) L. J. Prins, J. Huskens, F. De Jong, P. Timmerman and D. N. Reinhoudt, *Nature*, 1999, **398**, 498; (*b*) K. A. Jolliffe, M. Crego Calama, R. Fokkens, N. M. M. Nibbering, P. Timmerman and D. N. Reinhoudt, *Angew. Chem., Int. Ed.*, 1998, **37**, 1247; (*c*) M. Crego Calama, R. Fokkens, N. M. M. Nibbering, P. Timmerman and D. N. Reinhoudt, *Chem. Commun.*, 1998, 1021; (*d*) P. Timmerman, R. H. Vreekamp, R. Hulst, W. Verboom, D. N. Reinhoudt, K. Rissanen, K. A. Udachin and J. Ripmeester, *Chem. Eur. J.*, 1997, **3**, 1823; (*e*) R. H. Vreekamp, J. P. M. van Duynhoven, M. Hubert, W. Verboom and D. N. Reinhoudt, *Angew. Chem., Int. Ed. Engl.*, 1996, **35**, 1215.

15 K. A. Jolliffe, P. Timmerman and D. N. Reinhoudt, *Angew. Chem., Int. Ed.*, 1999, **38**, 933.

16 (*a*) M. Holtz, X. Mao, D. Seiferling and A. Sacco, *J. Chem. Phys.*, 1996, **104**, 669; (*b*) A. R. Waldeck, P. W. Kuchel, A. J. Lennon and B. E. Capman, *Prog. Nucl. Magn. Reson. Spectrosc.*, 1997, **30**, 39.

17 J. P. Mathias, E. E. Simanek, J. A. Zerkowski, C. T. Seto and G. M. Whitesides, *J. Am. Chem. Soc.*, 1994, **116**, 4316.

18 C. M. Marjo, F. De Jong, P. Timmerman and D. N. Reinhoudt, unpublished results.

19 R. H. Vreekamp, W. Verboom and D. N. Reinhoudt, *Recl. Trav. Chim. Pays-Bas*, 1996, **115**, 363.

20 M. Sato and S. Ebine, *Synthesis*, 1981, 472.

21 H. R. Ing and R. F. H. Manske, *J. Chem. Soc.*, 1926, 2348.

22 J.-D. van Loon, A. Arduini, L. Coppi, W. Verboom, A. Pochini, R. Ungaro, S. Harkema and D. N. Reinhoudt, *J. Org. Chem.*, 1990, **55**, 5639.

23 C. T. Seto, J. P. Mathias and G. M. Whitesides, *J. Am. Chem. Soc.*, 1993, **115**, 1321.

24 L. J. Prins, K. A. Jolliffe, K. A. Hulst, P. Timmerman and D. N. Reinhoudt, *J. Am. Chem. Soc.*, 2000, **122**, 3617.

25 J.-A. Perez-Aldemar, H. Abraham, C. Sanchez, K. Rissanen, P. Prados and J. de Mendoza, *Angew. Chem., Int. Ed. Engl.*, 1996, **35**, 1009.

26 J. A. Zerkowski, J. C. MacDonald, C. T. Seto, D. A. Wierda and G. M. Whitesides, *J. Am. Chem. Soc.*, 1994, **116**, 2382.

27 C. T. Seto and G. M. Whitesides, *J. Am. Chem. Soc.*, 1993, **115**, 905.

28 A. Casnati, M. Fochi, P. Minari, A. Pochini, M. Reggiani, R. Ungaro and D. N. Reinhoudt, *Gazz. Chim. Ital.*, 1996, **126**, 99.

29 Quanta 97, Molecular Simulations, Waltham, USA.

30 (*a*) B. R. Brooks, R. E. Bruccoleri, B. D. Olafson, D. J. States, S. Swaminathan and M. Karplus, *J. Comput. Chem.*, 1983, **4**, 187; (*b*) F. A. Momany, V. J. Klimkowski and L. Schäfer, *J. Comput. Chem.*, 1990, **11**, 654; (*c*) F. A. Momany, R. Rone, H. Kunz, R. F. Frey, S. Q. Newton and L. Schäfer, *J. Mol. Struct.*, 1993, **286**, 1.